

Adaptive Aggregation of Peptide Model Systems

Juhyon J. Lee, Merwe Albrecht,[†] Corey A. Rice,[‡] and Martin A. Suhm*

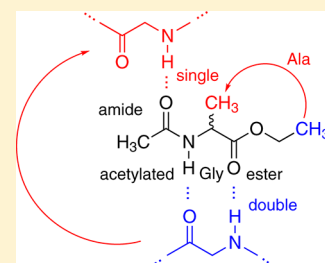
Institut für Physikalische Chemie, Universität Göttingen, Tammannstraße 6, 37077 Göttingen, Germany

Anke Stamm, Manuel Zimmer, and Markus Gerhards*

Fachbereich Chemie and Research Center OPTIMAS, Physikalische und Theoretische Chemie, TU Kaiserslautern, Erwin-Schrödinger-Straße 52, 67663 Kaiserslautern, Germany

Supporting Information

ABSTRACT: Jet-cooled infrared spectra of acetylated glycine, alanine, and dialanine esters and their dimers are reported in the amide A and amide I–III regions. They serve as particularly simple peptide aggregation models and are found to prefer a single backbone conformation in the dimer that is different from the most stable monomer backbone conformation. In the case of alanine, evidence for topology-changing chirality discrimination upon dimer formation is found. The jet spectroscopic results are compared to gas phase spectra and quantum chemical calculations. They provide reliable benchmarks for the evaluation of the latter in the field of peptide interactions.



1. INTRODUCTION

Protein–protein interactions rely on molecular recognition between and correct torsion of specific amino acid sequences, which needs to be modeled accurately.¹ For the purpose of quality assessment in molecular modeling and quantum chemistry, it is desirable to experimentally characterize such interactions at the most elementary protected amino acid level in the gas phase, cf., e.g., refs 2–6. In contrast to solution⁷ and matrix isolation⁸ studies, gas phase investigations allow for a direct comparison to theoretical spectra without environmental shifts and to predicted conformational energy sequences.⁹ This is particularly true for the lowest energy conformations¹⁰ and for those stabilized by high barriers, whereas other cases may profit from matrix isolation.¹¹ To induce aggregation, low temperature nonequilibrium measurements are necessary. There has been tremendous success in this field using IR spectroscopic techniques for neutral amino acids and peptides in supersonic jets combined with thermal or laser desorption (cf., e.g., refs 2–6 and 12–34) providing detailed insights into the intermolecular forces underlying folding and aggregation events. Almost invariably, these techniques rely on an aromatic chromophore and would thus have to involve VUV excitation for the simplest amino acids such as glycine and alanine, unless these are modified with an aromatic substituent.^{22,31} Here, we start to fill this gap using FTIR spectroscopy of thermally evaporated and adiabatically reagggregated acetylated amino acid esters in pulsed supersonic jet expansions, in combination with equilibrium gas phase investigations of the monomers. This is a continuation of the study of very elementary peptide motifs in the gas phase³⁵ that focused on the amide group alone and its aggregation preference. Here, we concentrate on glycine and alanine, the two simplest protein building blocks.

In contrast to amino acid esters with a free amine end group,³⁶ the NH group becomes a strong hydrogen bond donor when an acetyl residue is attached to it. This is a consequence of sp^2 hybridization.³⁷ It reduces the volatility and turns on peptide-like intermolecular interactions. Furthermore, the resulting structural motif can be found in depsipeptides (peptolides), which contain not only amide but also ester bonds.³⁸ The commercially most prominent example may be the methyl ester of L-aspartyl-L-phenylalanine (aspartame), a popular sweetener. In contrast to unprotected amino acids (cf., e.g., refs 15, 17, 25, 39, and 40), an extremely low vapor pressure is not an issue for acetylated esters, such that prolonged heating to generate on the order of 100 Pa of the compound in the gas phase is feasible.

One of the simplest homologues is N-acetylglycine ethyl ester (Ac-Gly-OEt) (Figure 1). By exchanging one of the C_α hydrogens with the methyl group of the ester, one arrives at the two (D/L) enantiomeric Ac-Ala-OMe (N-acetylalanine methyl ester) forms. Their chirality-sensitive aggregation will be the subject of the present contribution. Furthermore, we investigate the proteinogenic (LL) form of the dialanine methyl ester Ac-Ala-Ala-OMe.

A key purpose of this study is to provide benchmarks for appropriate quantum chemical treatments of the conformational landscape and force field, which are also applicable to larger building blocks. When aiming at spectroscopically useful predictions, typical standard approaches have serious draw-

Special Issue: Joel M. Bowman Festschrift

Received: January 3, 2013

Revised: February 15, 2013

Published: March 12, 2013

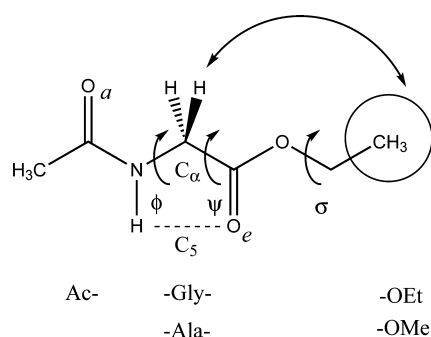


Figure 1. Torsional angles ϕ , ψ , and σ defining the conformations of Ac-Gly-OEt and Ac-Ala-OMe (exchanging the methyl group from the ester with one of the C_α hydrogen atoms). The two carbonyl groups are labeled a (amide) and e (ester), the weak $\text{HN}-\text{C}=\text{O}$ contact with C_5 .

backs. The harmonic B3LYP hybrid density functional approach provides an economic representation of fundamental vibrations and their hydrogen bond-induced shifts, in part profiting from error compensation. However, it may fail in describing secondary, dispersion-driven interactions,⁴¹ the importance of which grows with the size of the system and may be decisive for chirality recognition phenomena.⁴² Pure density functionals like B97, when augmented by dispersion corrections,⁴³ are better suited for the latter problem, but the bonds are usually too soft and reactive to hydrogen bonds, thus overestimating frequency shifts. MP2 and higher order post-HF approaches require large basis sets or explicit correlation treatments to avoid artificial energy contributions and to provide reasonable force constants. In the present work, we will demonstrate some of these limitations for the investigated model systems and explore B3LYP-D3⁴⁴ as a valuable and scalable tool to describe such peptide interaction units.

2. METHODS

IR spectra of cold monomers and dimers were measured using the *popcorn-jet*.^{35,45–47} A helium gas pulse with a volume of about 1 standard liter and less than 1 s duration flows through a heated bed of about 10 g spherical molecular sieve loaded with ≈ 3 g of the protected amino acid, before it expands through two parallel 0.5 mm \times 10 mm slits into a large vacuum chamber. During the peak flow, two 2 cm^{-1} resolution Bruker IFS 66v/S FTIR scans are collected by focusing the IR beam perpendicular to the two slits at a distance of about 5 mm and recording the feeble absorption with a large area InSb photovoltaic or HgCdTe photoconductive detector. Due to a slit separation of 10 mm, the IR radiation samples two weakly interacting expansions, thus essentially doubling the molecular column density. The vacuum chamber is large enough to prevent a pressure rise above 60 Pa during the pulse. After the chamber is evacuated for 40 s down to a pressure of less than 20 Pa, the next gas pulse is probed. In the waiting time, two poppet valves enclose the heated molecular sieve. Typically, the spectra are block-averaged over 50 gas pulses (corresponding to a consumption of about 0.2–0.4 g of the ester) and several such blocks are combined in the spectra shown. A few interferograms containing spikes due to electronic perturbations were removed from the averaging process. Further experimental details can be found in ref 48.

The equilibrium gas phase FTIR spectra of acetylated L-alanine and di-L-alanine methyl ester were measured in a Bruker

Vertex 80v FTIR spectrometer by using a self-constructed heatable cell (similar to the one of ref 39). The chosen aluminum cell is 95 mm long and has a diameter of 30 mm. At both ends CaF_2 windows are attached. The cell is heated by 16 resistors (each 3.3 Ω). The substance is placed in a ball valve fixed on top of the cell. A rotary vacuum pump constantly evacuates the heated cell, resulting in a pressure of 1–0.1 Pa. After a background spectrum is taken, the vacuum pump is closed and the ball valve is opened for a short time; thus, the substance is able to drop down into the cell. Due to the strong change in pressure and temperature, the substance sublimates directly without decomposition. The IR spectra are measured with a HgCdTe photoconductive detector (cooled with liquid nitrogen to 77 K); an average of 50 spectra at a resolution of 1 cm^{-1} is recorded.

Acetylglycine ethyl ester (Ac-Gly-OEt, CAS number: 1906-82-7, 98%, Sigma-Aldrich, bp 260 $^\circ\text{C}/0.95$ bar according to supplier), acetyl-L-alanine methyl ester (Ac-Ala-OMe, CAS number: 3619-02-1, >99%, Bachem), acetyl-D-alanine methyl ester (Ac-D-Ala-OMe, CAS number: 19914-36-4, >99%, Bachem), and acetyldi-L-alanine methyl ester (Ac-Ala-Ala-OMe, CAS number: 30802-26-7, >99%, Bachem) were used as supplied. The relative chirality of the D/L-Ala samples was verified by polarimetry in acetone solution. As the racemic mixture of acetyl-alanine methyl ester was not commercially available, we prepared equimolar mixtures on our own.

Accompanying quantum chemical calculations at the B3LYP^{49,50} and MP2⁵¹ level using the 6-311+G* basis set were carried out with the Gaussian 03 program suite.⁵² Test calculations were extended to the MP2/aug-cc-pVTZ level. The dispersion-corrected DFT-D2 results (B97D/TZVP/TZVPfit denfit) were obtained with Gaussian 09.⁵³ B3LYP-D3/TZVP calculations were carried out with TURBOMOLE with BJ-Damping as implemented in TURBOMOLE.⁵⁴

Two independent strategies were employed for the conformational landscape search of the dimers prior to quantum chemical optimization. An intuitive approach guided by a maximization and permutation of hydrogen bonds with variation of soft torsional angles and a more systematic approach based on the CFF force field, which has been used as implemented in the Discovery studio.⁵⁵ The CFF force field was used to independently cross-check the former approach for completeness. For dimers involving two strong hydrogen bonds, no missing conformations were revealed, whereas some of the less intuitive structures involving only one dominant hydrogen bond and several weaker interactions were only located by the systematic approach. In a final stage, selected transformations of converged dimer structures between Ac-Gly-OEt, Ac-D-Ala-OMe and Ac-L-Ala-OMe were carried out to ensure a gap-free coverage of the low energy conformations.

With CFF, a class II force field with anharmonic terms and cross-terms was employed. First of all, the conformational landscape of the system of interest was scanned by a modified quenched dynamics technique: Beginning with an arbitrary starting geometry, a short-time molecular dynamics run (typically about 2 ps for the heating dynamics and 5 ps for slight cooling dynamics with 1 fs time-step) was performed with certain initial and target temperatures. The final geometry was fully optimized and stored for a later analysis. This minimized structure was reheated to the target temperature and another short-time dynamics run was added. This procedure was executed until a desired ensemble of minimized structures

was found. All minima were sorted with respect to their relative energy.

The conformation of acetylated amino acid esters (Figure 1) can be characterized by the N–C_α torsional angle ϕ and the C_α–C torsional angle ψ ,^{2,56,57} as well as an additional O–C torsional angle σ in the case of ethyl esters. We encode these two (three) angles by a sequence of two (three) labels ab (abc) and translate the code into the traditional greek letter peptide nomenclature,^{2,56–58} where appropriate. The parallel use of both nomenclatures facilitates the connection of the peptide research field to a wide range of conformational studies of related compounds. A translation table is given in the Supporting Information (Table S1). Rotamerization around the amide or ester bonds is neglected, unless stated otherwise. In the case of dialanine, two sets of $\phi\psi$ labels are used, starting from the acetylated N-terminus.

In the case of glycine, we qualitatively distinguish between trans = t ($180^\circ \pm 60^\circ$) and gauche = g ($60^\circ \pm 60^\circ$) torsional angles and denote a g angle of opposite helicity in the same monomer or dimer with g'. In the case of alanine, we provide explicit (\pm) signs for the g (and in some cases t) angles because of the diastereomeric relationship to the asymmetric carbon center.⁵⁹ If not indicated otherwise, Ala denotes L-alanine.

3. RESULTS AND DISCUSSION

3.1. Protected Glycine Monomer. The jet FTIR spectrum of N-acetylglycine ethyl ester shows a single narrow NH stretching band (Figure 2, trace a) at 3464 cm⁻¹ and two

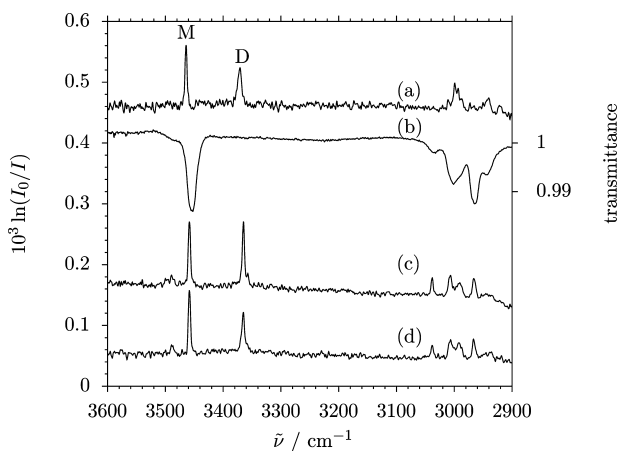


Figure 2. Infrared spectra of different peptide models in the NH stretching region, clearly separating monomer (M) and dimer (D) contributions: (a) Ac-Gly-OEt (300 jet pulses, $T_{\text{substance}} = 363$ K); (b) gas phase transmittance spectrum of Ac-Ala-OMe at 343 K; (c) Ac-Ala-OMe (600 jet pulses, $T_{\text{substance}} = 353$ K); (d) racemic Ac-Ala-OMe (600 jet pulses, $T_{\text{substance}} = 353$ K).

prominent C=O stretching bands (Figure 3, trace a) at 1759 cm⁻¹ (ester C=O) and 1714 cm⁻¹ (amide C=O), which may be explained by a single isolated, cold Ac-Gly-OEt monomer conformation. This observation can be reconciled with earlier experimental evidence. A microwave study⁶⁰ found two isomers with planar peptide backbone (β or tt conformation, stabilized by an internal C₅ hydrogen contact) differing in the ester torsional angle σ (g/t). This torsional isomerism is not expected to affect the NH and C=O functional groups in a significant way, so the lower resolution IR spectra of these ethyl

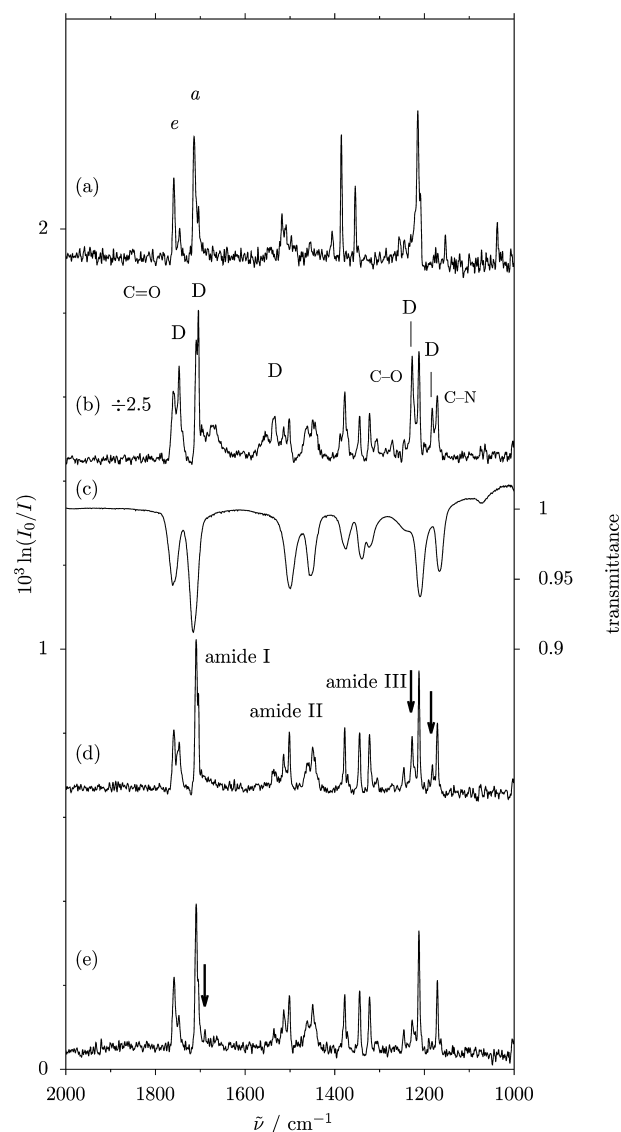


Figure 3. Infrared spectra of different peptide models in the C=O and fingerprint region: (a) Ac-Gly-OEt (300 jet pulses, $T_{\text{substance}} = 363$ K); (b) Ac-Ala-OMe (149 jet pulses, $T_{\text{substance}} = 353$ K, high sample concentration, intensity divided by 2.5, prominent dimer bands marked D); (c) gas phase transmittance spectrum of Ac-Ala-OMe at 343 K; (d) Ac-Ala-OMe (978 jet pulses, $T_{\text{substance}} = 343\text{--}353$ K, low sample concentration); (e) racemic Ac-Ala-OMe (610 jet pulses, $T_{\text{substance}} = 353$ K). Arrows mark spectral features indicative of topology-changing chirality recognition.

group rotamers are likely to overlap and are therefore consistent with the microwave evidence.

IR spectra recorded in CCl₄ solution at room temperature show NH and C=O stretching bands of solvated monomers at 3442 and 1745/1691 cm⁻¹, respectively.⁷ The red shifts of 14–23 cm⁻¹ relative to the jet spectrum are a result of solvation and thermal excitation. A weak band at 3465 cm⁻¹ due to N–H groups without intramolecular C₅-type interaction may correlate with a weak 3491 cm⁻¹ feature in the jet at higher concentration (Figure S1 in the Supporting Information). However, this is also the region of C=O overtones. The ratio to the ester C=O fundamental is 1.985 in the jet and 1.986 in CCl₄ solution, which is very close to the ratio of 1.986 between the C=O overtone and fundamental of glycine ethyl ester.³⁶

We note that analogous spectra have been obtained for the dominant β isomer of the $-\text{NH}(\text{CH}_3)$ protected glycine Ac-Gly-NHMe as monomer in dichloromethane solution and in rare gas matrices.⁸ The relevant NH stretching band is assigned at 3419 cm^{-1} (dichloromethane) and about 3425 cm^{-1} (Ar, Kr matrix). Due to the solvent shift and the different electronic properties of the $-\text{NHMe}$ group, this brings the glycine NH stretching fundamental into Fermi resonance with the amide $\text{C}=\text{O}$ stretch overtone, a situation which is not evident in the esters investigated here. The $\text{C}=\text{O}$ stretching region is further complicated by the similarity of the two carbonyl oscillators in Ac-Gly-NHMe, both being part of an amide group, and the existence of a competing conformer.

Therefore, the case of Ac-Gly-OEt provides a simpler entry point into the conformational analysis of protected peptide models, as in the case of Ac-Phe-OMe.² However, the rationalization of the simple spectral features with specific quantum chemical predictions of the conformers is surprisingly complex. Several of these conformers have been investigated at the MP2/6-311G** level in the microwave study⁶⁰ and it was found that the ester *g/t* energy sequence is inverted with respect to the experiment. The latter unambiguously shows the *t* structure to be the most stable. Our own investigations at the slightly different MP2/6-311+G* level rectify this and predict *tt-t* to be more stable than *tt-g*, but they reveal a surprising effect for the peptide backbone. *gt-t* (ϵ) type conformations are found to be competitive, which is clearly not the case at the MP2/aug-cc-pVTZ or the various DFT levels (Figure 4 and Supporting Information, Table S2 and Figure S3). We speculate that the partially folded ϵ structure profits from basis set superposition but the main message is that the

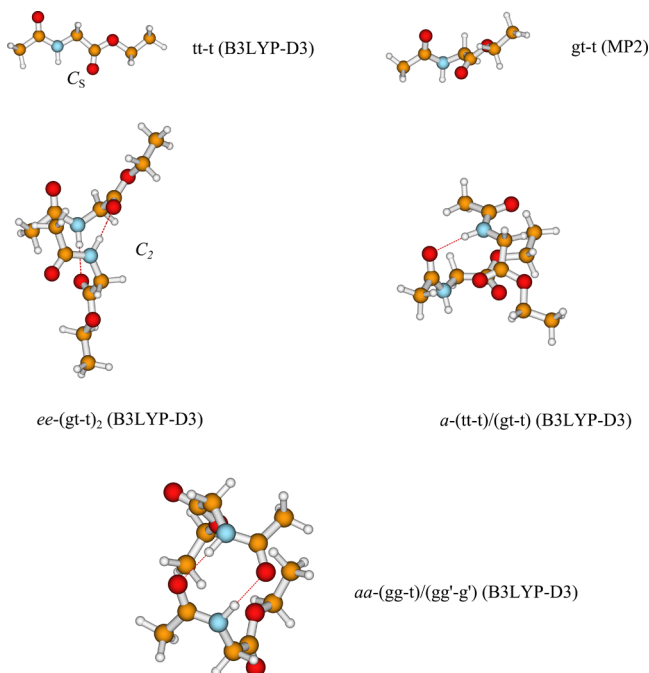


Figure 4. Ac-Gly-OEt monomer global minimum structures according to B3LYP-D3 (*tt-t*) and MP2 calculations (*gt-t*, artificially stabilized by basis set incompleteness) and the realization of the latter conformation in the stable symmetric dimer. Note that there is a nearly isoenergetic unsymmetric structure *a-(tt-t)/(gt-t)* involving a single hydrogen bond to an amide $\text{C}=\text{O}$. Dimers such as *aa-(gg-t)/(gg'-g')* can only be realized with *cis*-amide monomers and are much higher in energy.

potential energy hypersurface of acetylated amino acid esters is rather flat along the ϕ angle, a property that will turn out to be important in the dimers. Concerning the computationally less expensive density functional based calculations, they differ in the ethyl ester group preference. The B3LYP prediction and its D3-augmented variant are consistent with the microwave observation of a more stable *trans* conformation, whereas the B97D prediction is more ambiguous, as in the case of menthol.⁶¹

In terms of spectral predictive power, the harmonic NH stretching wavenumber for the *tt-t* monomer is 149 (B3LYP), 145 (B3LYP-D3), 181 (MP2), and 75 cm^{-1} (B97D) too high, when compared to the experimental anharmonic value of 3464 cm^{-1} (Supporting Information, Table S3). Considering an effective diatomic anharmonicity constant $\omega_e x_e$ of the NH stretching mode on the order of 70 cm^{-1} ,^{62–64} B3LYP(-D3) is thus probably closest to the true harmonic prediction, followed by MP2. The B97D potential is seen to be significantly too soft, which should be kept in mind when looking at hydrogen bond-induced shifts. This is also true for the $\text{C}=\text{O}$ stretching modes (Supporting Information, Table S4), which are harmonically predicted 1–2% too high by MP2 and B3LYP calculations, as they should, whereas the B97D prediction is already too low, without including anharmonicity.

The presence of folded backbone conformations in solution or in the gas phase is easy to diagnose from the IR spectrum. Harmonic predictions for the NH stretching mode locate all backbone-folded structures at least 10 cm^{-1} (more typically $20\text{--}30\text{ cm}^{-1}$) blue-shifted relative to the *tt* structures, whereas the change in σ (ester group) torsional angle changes the wavenumber by less than 2 cm^{-1} . The most visible folded isomers in terms of NH stretching intensity are those that conserve the C_5 intramolecular hydrogen contact (*tg* or δ), but *gg* (α) isomers or clusters cannot be ruled out as the origin of the weakly observed blue-shifted NH stretching band, either. In the carbonyl range, qualitatively similar but quantitatively smaller blue shifts are predicted for folded isomers. They are not evident in the experimental spectra, again ruling out significant contributions at least under jet-cooled conditions. Theory is unambiguous in assigning the higher frequency carbonyl stretching band to the ester group (ϵ), whereas the more intense lower frequency band originates from the amide group (α).

Structural, energetic, and spectral predictions for a range of Ac-Gly-OEt monomer conformations can be found in the Supporting Information (Tables S2–S4, Figure S3). Deviations of the *tt-t* structure from exact C_5 -symmetry at the MP2 level are likely due to basis set incompleteness. This is suggested by the aug-cc-pVTZ results, which predict a C_5 -symmetric global minimum, like all other calculations. It would be difficult to rule out the artificial MP2 *gt* (ϵ) structures based only on their infrared NH stretching spectra, but microwave spectroscopy⁶⁰ and higher level calculations clearly show that they may be disregarded for monomeric Ac-Gly-OEt.

In summary, the only rotamerism in jet-cooled and room temperature *N*-acetylglycine ethyl ester is the relative position of the ethyl ester group, whereas the peptide-mimetic backbone is clearly planar (β , C_5 -stabilized, *tt*), but rather flexible along the nonamide $\text{N}-\text{C}$ bond torsion ϕ .

3.2. Protected Glycine Dimer. The jet spectrum of Ac-Gly-OEt (Figure 2, trace a) features an additional band in the NH stretching region. It is broader, centered at 3372 cm^{-1} , and grows faster with concentration than the monomer band

(Supporting Information, Figure S1). It is straightforward to assign to hydrogen-bonded dimers of the protected glycine. Corresponding C=O stretching bands appear as less prominent red-shifted satellites to the monomer transitions, at 1746 and 1704 cm^{-1} (Figure 3 and Supporting Information, Figure S2). Red shift (92 cm^{-1}) and intensity are more pronounced for the NH stretching band, as expected for a hydrogen-bonded species. The FTIR technique lacks size-selectivity; therefore, it cannot be ruled out that there are weak dimer components underneath the monomer bands in either spectral range.

The jet observations find qualitative parallels in the solution spectra at moderate concentrations.⁷ There, the NH red shift for the dimeric aggregate is only 72 cm^{-1} instead of 92 cm^{-1} , which is easily explained by thermal weakening of the hydrogen bonds and preferential interaction of the solvent with the more accessible monomer NH group. A high-concentration feature which is 61 cm^{-1} further red-shifted corresponds nicely to the jet feature which is about 50 cm^{-1} more red-shifted and must be attributed to larger aggregates. The more subtle C=O stretching shifts upon dimerization are less systematic. For the ester C=O group, the jet observation of a 13 cm^{-1} dimerization red shift is to be contrasted to a 8 cm^{-1} blue shift in CCl_4 solution,⁷ although a broadening of the solution band complicates the precise band center assignment. For the amide group, the correspondence between the 10 (jet) and 20 cm^{-1} (solution) dimerization red shifts is at least qualitatively better. It appears that the jet-cooled dimers involve mostly the ester carbonyl group, whereas this is less likely in solution.

While the low temperature experiment is consistent with one dominant hydrogen-bonded dimer structure (apart from ester group rotamerism), the situation in solution may be more complex. As there are no microwave data for the dimer, quantum chemical calculations should be consulted to shed further light on the structural issue in the gas phase. The limitations observed for the monomer should be kept in mind.

Dimers with one or two intermolecular NH hydrogen bonds can involve amide (*a*) or ester (*e*) carbonyl groups as acceptors in different combinations. All four theoretical approaches agree in finding *gt* (*e*) and *tt* (*β*) monomer backbones among the four most stable dimer structures (Supporting Information, Table S5).

Beyond this point, the quantum chemical dimer predictions are diverse, but all agree in predicting close competition between a C_2 -symmetric pairing of the two *gt* (*e*) backbones via the ester groups (*ee*) and a single amide C=O bonded form (*a*) augmented by secondary stacking interactions (Figure 4). This is interesting, because *ee* stands for a β -sheet motif, whereas *a* is reminiscent of the α -helical environment. At the MP2 and B3LYP-D3 level, the amide coordination wins by a small margin, whereas B3LYP and B97D predict a preference for *ee*. At B97D, even the ester ethyl conformation can be changed before the amide-bonded structures come into play, but this is in part an artifact of the B97D underestimation of ester *g/t* isomerization. An inversion-symmetric *ee* arrangement (C_i) cannot compete with the C_2 -symmetric structure, probably because it does not allow for additional stacking interactions between the amide groups (Figure S4, Supporting Information). Stacking of the ester groups appears to be the driving force for the amide-coordinated dimer. MP2, B97D, and B3LYP-D3 prefer the donor molecule in the stretched β -form, whereas B3LYP prefers the acceptor molecule in this conformation.

One may ask why *aa*-type dimers involving two NH hydrogen bonds to amide C=O are not found to be stable. After all, a comparison of the dimer of *N*-methyl acetamide with a complex between *N*-methyl acetamide and methyl acetate reveals that the corresponding $\text{N-H}\cdots\text{O}=\text{C}_a$ hydrogen bond is 20–30% more stable than a $\text{N-H}\cdots\text{O}=\text{C}_e$ hydrogen bond. The energy required to form two *cis*-amide conformations, which then enables formamide-like pairing of two units,⁶⁵ is probably too high. This thermodynamic argument is enhanced by kinetic control in the case of a jet expansion, because the barrier for *trans/cis* isomerization is very high. Furthermore, one may expect a more pronounced red shift in this case. Indeed, the best *cis*-amide dimer structure we could find ((*gg-t*)/(*gg'-g'*)) (Figure 4) is not compatible in terms of energy and spectrum (see later section and Table S5, Supporting Information).

The gas phase *ee*-dimerization energy for two *tt-t* units including the effect of zero point vibration varies widely among the methods, as expected. The B3LYP dissociation energy result for (*gt-t*)₂ of 27 kJ mol^{-1} misses out dispersion contributions whereas the MP2 result of 67 kJ mol^{-1} overestimates them and suffers from basis set superposition error. The B97D and B3LYP-D3 results of 49 and 56 kJ mol^{-1} should be in the correct range. We find that this is about twice the dissociation energy of the complex between *N*-methylacetamide and methyl acetate, which may serve as a model for one of the (*gt-t*)₂ hydrogen bonds. The reason for the apparent additivity is a compensation between two effects. On the one hand, the *tt-t* monomer already contains a weak intramolecular hydrogen contact, which is broken upon dimerization. On the other hand, less directed polar and dispersive forces act in the dimer to lower its energy relative to two monomers. In solution (ref 7 and references cited therein), only about half of the binding energy survives due to thermal weakening and solvent competition.

In view of the close energetic competition between *ee*- and *a*-bonded dimers at all levels, one may expect that experimental spectra provide a decision. In Figures 5 and 6, the experimental NH and C=O jet spectra are compared to harmonic simulations, assuming a uniform bandwidth of 5 cm^{-1} (fwhm). Included in the simulation are equal proportions of *tt-t* and *tt-g* monomers as well as 10 times fewer *ee*-dimers (*gt-*

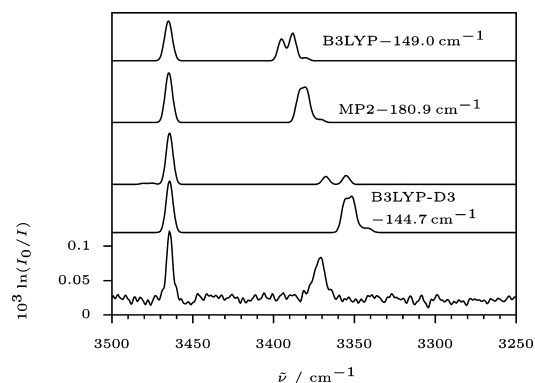


Figure 5. Simulated spectra for Ac-Gly-OEt (monomers *tt-t*, *tt-g* and dimers (*gt-t*)₂, (*gt-g*)₂ (for B3LYP-D3 alternatively (*tt-t*)/(*gt-t*), (*tt-t*)/(*gt-g'*), above the label)) in the NH stretching region at the B3LYP/6-311+G*, MP2/6-311+G*, and B3LYP-D3/TZVP levels compared to the experimental spectrum (bottom trace) shown in trace a of Figure 2.

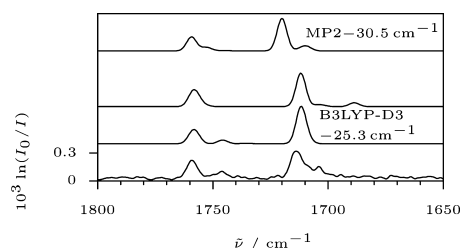


Figure 6. Simulated spectra for Ac-Gly-OEt (monomers tt-t, tt-g and dimers (gt-t)₂, (gt-g)₂ (for B3LYP-D3 alternatively (tt-t)/(gt-t), (tt-t)/(gt-g'), above the label)) in the C=O stretching region at the MP2/6-311+G* and B3LYP-D3/TZVP levels compared to the experimental spectrum (bottom trace) shown in trace a of Figure 3.

t)₂ and (gt-g)₂. In the B3LYP-D3 case, we offer an alternative 10% contribution of two *a*-dimers in a second trace. Note that the spectra involve a single intensity scaling for both spectral ranges but use individual shifts of the bands such that the experimental monomeric NH stretching and ester C=O stretching band positions for tt-t are always reproduced (accounting in first order for anharmonicity and other deficiencies in the harmonic predictions for a given functional group). The B97D simulation is omitted due to its severe overestimation of shifts (Table S6 in the Supporting Information). Figure 5 shows that *a*-dimers have a much inferior band intensity and thus visibility in the NH stretching range, whereas the C=O stretching spectra in Figure 6 (see also Supporting Information, Table S7) seem to rule out a dominant contribution of such *a*-dimers. Rewardingly, the relative C=O and NH intensities of the monomer match well, which helps in quantifying the dimer contributions. We estimate about 10% *ee*-dimers and less than 5% *a*-dimers in the expansion. In detail, the B3LYP calculations underestimate the N–H dimerization shift, whereas the B3LYP-D3 calculations overestimate it. Even the increased width of the dimer signal is explained by a slight mismatch of the ester g/t-isomers. In the C=O stretching range (Figure 6), the dimer intensities and shifts are best reproduced at the B3LYP-D3 level, except for the amide C=O shift, which is too large for *ee* and too small for *a*.

The solution data are actually more consistent with amide dimer structures, where a strong intermolecular hydrogen bond to the amide C=O releases one of the ester C=O groups from a weak intramolecular C₅ contact. Indeed, such a structure has been proposed before.⁷

In summary, acetylglycine ethyl ester switches from its all-*trans* (t, C₅ or β) monomer conformation into a kinked (gt or ε) structure when forming a hydrogen-bonded dimer. The most stable dimer consists of two conformationally homochiral monomer units connected via NH hydrogen bonds to the ester carbonyl groups and has C₂ symmetry. Single hydrogen bonds to the amide C=O may not be far away in energy, as indicated by the computational and spectroscopic results. We will see that for alanine this competition is activated in a chirally selective way. A solvent as inert as CCl₄ also appears to switch to such singly hydrogen-bridged dimers.⁷

3.3. Protected Alanine Monomer. When one of the two C_α hydrogens in Ac-Gly-OEt is formally exchanged with the terminal ester methyl group, one of the enantiomers of Ac-Ala-OMe, the simplest ester of acetylated alanine, is created. The biologically most abundant form is the proteinogenic L-alanine, but bacteria exploit the resistance of the D-form against

common proteases in their cell walls. For an isolated molecule, there is no difference in the rotational or vibrational spectra apart from subtle parity violation effects.^{66,67}

It was shown by microwave spectroscopy that Ac-Ala-OMe exists essentially in a single conformation in a supersonic jet.⁶⁸ It corresponds to the most stable form of Ac-Gly-OEt, with all backbone atoms close to a plane and a weak C₅ intramolecular interaction. Depending on the handedness of the asymmetric C_α it may be denoted t–t+ (β_L) or t+t– (β_D).

As shown in Figure 2 (trace c), the NH stretching spectrum in the jet is consistent with such a single dominant monomer, with a strong and narrow band at 3459 cm⁻¹.

At thermal equilibrium around 343 K (trace b of Figure 2), the dominant band maximum shifts by –4 cm⁻¹ to 3455 cm⁻¹ and there is still a rather weak shoulder near 3483 cm⁻¹, but also on the low-wavenumber slope. This supports a monomer interpretation, because dimers are not stable under such conditions.

The NH stretching band of Ac-Ala-OMe has been observed before in CH₂Cl₂,⁶⁹ with a solvent red shift of 26 cm⁻¹ for the C₅ conformation, similar to that observed for Ac-Gly-OEt. Solvent effects of this size⁷⁰ mask the glycine/alanine substitution shift on the NH stretching wavenumber, which amounts to –5 cm⁻¹ on the basis of the jet spectra and may be attributed to an inductive effect of the C_α methyl group, possibly combined with distortion of the intramolecular C₅ contact due to the backbone departure from planarity. An earlier study of Ac-Ala-OMe in CHCl₃ is consistent with the CH₂Cl₂ results.⁷¹

The C=O stretching region has also been investigated by a range of techniques. The two monomer-based peaks in the jet spectrum are found at 1759 (ester) and 1709 cm⁻¹ (amide), very close to the Ac-Gly-OEt values. The ratio of 1.984 of the weak band in the NH stretching region to the ester fundamental again suggests a C=O overtone interpretation of the former. In the high temperature gas phase (spectrum c in Figure 3), the C=O stretching fundamentals occur at 1760 and 1716 cm⁻¹. The unusually large 7 cm⁻¹ blue shift of the amide C=O relative to the jet spectrum provides evidence for the weak intramolecular C₅ interaction, which is thermally broken at and above room temperature. Diluted in CH₂Cl₂, these bands are red-shifted by 17 and 29 cm⁻¹, respectively.⁶⁹ The shifts are comparable to the bandwidths in solution. The relative similarity of the Ac-Gly-OEt/Ac-Ala-OMe monomer spectra extends to the C-terminal amide substituted Ac-Ala-NHMe.⁸ Also shown in Figure 3 is the conformation-sensitive amide III region together with the amide II bands for the esters.⁷² It is evident from a comparison of traces a and d that this fingerprint domain of the IR spectrum reacts strongly on the introduction of a methyl group at C_α. We refrain from a detailed assignment at this stage but come back to this region when discussing dimers.

The next step is to verify whether the conformational dominance observed in the monomer spectra is confirmed by quantum chemical calculations. This is the case for the B3LYP(-D3) and B97D DFT-based calculations (Table S8 in the Supporting Information). All predict a tt (more precisely t–t+) or β_L conformation for the L-form separated by at least 8 kJ mol⁻¹ from the next two (t–g– and g–g–) conformations. Only at the MP2/6-311+G* level is there a closer-by g–t+ or ε_L structure (Figure S7 in the Supporting Information), reminiscent of the Ac-Gly-OEt gt case. It is about 2 kJ mol⁻¹ higher in energy than the global minimum and collapses into

the tt conformer for the B3LYP(-D3) and B97D calculations. As in the glycine case and like the low-lying lg-g- conformer, it must be an artifact of the small basis set, but as we will see, it again adopts the preferred homodimer conformation. It remains stable at the MP2/aug-cc-pVTZ level but is now 5 kJ mol⁻¹ higher in energy.

At the B3LYP(-D3) level, the harmonic N-H stretching wavenumber decreases somewhat when moving from Ac-Gly-OEt to Ac-Ala-OMe except for lg+g+ (Table S9 in the Supporting Information). Experimentally, the decrease amounts to 5 cm⁻¹, which the MP2 and B97D calculations fail to predict even qualitatively. The predicted C=O stretching shifts relative to Ac-Gly-OEt (Table S10 in the Supporting Information) range between -2 and -5 cm⁻¹, in qualitative agreement with experiment (0 to -5 cm⁻¹).

In summary, the essentially monoconformational preparation of Ac-Ala-OMe evident in the spectrum is confirmed by quantum chemical calculations, but variations in the different levels indicate a facile distortion around the nonamide N-C bond, which prepares the molecule for intermolecular hydrogen bonding.

3.4. Protected Alanine Dimer. Enantiopure Ac-Ala-OMe expansions show a strong, narrow band in the NH stretching region at 3365 cm⁻¹ (Figure 2, trace c), which can be assigned to a dimer and corresponds to a hydrogen bond-induced red shift of 94 cm⁻¹. The narrowness in comparison to the dimer of Ac-Gly-OEt is attributed to the absence of ester conformational isomerism. A weak satellite band is slightly further red-shifted, at 3358 cm⁻¹. The C=O stretching bands assignable to small aggregates (Figure 3, compare traces b and d; see also Figure S6 in the Supporting Information) are red-shifted relative to their monomer counterparts, by 12 cm⁻¹ in the ester case and by only 4 cm⁻¹ in the amide case. Concentration-dependent bands assignable to dimers are also evident in the fingerprint region,⁶ and three particularly pronounced cases are marked D in Figure 3b.

If a racemic (L/D) mixture of Ac-Ala-OMe is expanded under nominally the same conditions, a very similar NH stretching spectrum is obtained (Figure 2, trace d), but the dimer band intensities are significantly lower. Possible interpretations are that the heteroconfigurational dimer composed of an L- and a D-form is less stable or less intensely absorbing than the homoconfigurational dimer. In the case of an analogous structure for a less stable heterochiral dimer, one would expect a reduced red shift for the heterochiral component. If the heterochiral structure were different, an additional band would also be predicted. Neither is the case, indicating coincidental band overlap. A less probable explanation is a reduced vapor pressure of the racemate, which crystallizes in nonracemic (2:1) strands of left- and right-handed molecules,⁷³ similar to racemic methyl mandelate.⁴¹ It is noteworthy that these crystal strands are built from the somewhat stronger NH hydrogen bonds to amide carbonyl groups. This is not an option for the isolated Ac-Ala-OMe dimer, if one wants to realize two intermolecular hydrogen bonds at the same time and if *cis*-amide formation is energetically or kinetically hindered.

The reduced spectral intensity of dimers in the racemic expansion is also evident in the C=O stretching region (Figure 3, compare traces d and e under similar expansion conditions and monomer abundances). In the enantiopure expansion, the stronger dimerization shift of the ester C=O group indicates its participation in the hydrogen bond instead of the better amide C=O acceptor group, which does not allow for double

hydrogen bonding without amide group torsion. In the racemic expansion, the sharp peak marked with an arrow in trace e is indicative of a significant fraction of well-defined amide hydrogen bonding. This supports the second interpretation of the racemic NH spectrum, namely a switch in hydrogen bond topology. Hydrogen-bonding to the C=O groups in the jet-cooled dimers also affects the 1200 cm⁻¹ region of the spectrum. Two prominently blue-shifted bands are observed. They correspond to mixed C-O and C-N single bond vibrations. The mixing is intensified compared to that for Ac-Gly-OEt. The strengthening of the C-O bond is a typical consequence of weakening the adjacent C=O bond, whereas the C-N bond defining the ϕ angle profits in a similar way from N-H bond elongation during hydrogen bonding. In the racemic expansion, the amount of ester C=O binding is clearly reduced, as are the dimer features in the 1200 cm⁻¹ region (marked with arrows in trace d). The situation for the amidic C=N bond in the amide II region is less obvious in terms of the direction of the shift, but clearly there is a dimer band in that region as well (compare traces b and d in Figure 3). All this points unambiguously to the involvement of the ester C=O group in hydrogen bonding of Ac-Ala-OMe to a second unit of the same chirality, whereas there is evidence for competitive amide bonding to a unit of opposite chirality.

To shed further light on this tentative experimental assignment, quantum chemical predictions of particularly stable dimer structures are indicated (Figure 7 and Tables S11 and S14 and Figures S8 and S9 in the Supporting Information). Among the homochiral dimers, the C₂ symmetric ester C=O bonded (lg-t)₂ or $\epsilon_L\epsilon_L$ dimer is by far the most stable. The monomer fragment is close in structure to the artificial MP2 monomer conformation and the binding energies including zero point energy correction range from 25 (B3LYP) over 51 (B97D) and 58 (B3LYP-D3) to 67 kJ mol⁻¹ (MP2), i.e., rather similar to the Ac-Gly-OEt case. The energy gap to the next-most stable homochiral dimers is larger than 10%, safely excluding a significant contribution by them in the jet spectra. We note that most metastable dimers are singly N-H hydrogen-bonded species, which also have an inferior IR visibility. They may contribute to the broad and weak signal below the dominant NH stretching wavenumber (Figure S5, Supporting Information). Most remarkably, the second-most stable dimer structure involves no intermolecular hydrogen bonds at all (Table S11, Supporting Information) but optimizes electrostatic and dispersion interactions in a sandwich-like structure. This emphasizes the uniqueness of the $\epsilon\epsilon$ -dimer motif.

The situation in the heteroconfigurational dimer case is radically different, as documented in the Supporting Information (Table S14 and Figure S9) and in Figure 7. On the energetically and spectrally most reliable B3LYP-D3 level, the strongest competitor to the homoconfigurational C₂-symmetric (lg-t)(lg-t) or $\epsilon_L\epsilon_L$ dimer is not the analogous C_i symmetric (lg-t)(dg+t) or $\epsilon_L\epsilon_D$ dimer. Indeed, it is less stable by about 6 kJ mol⁻¹. The reason is likely a lack of secondary amide stacking, as in the Ac-Gly-OEt case. On all levels except for B97D, more stable unsymmetrical dimers of the type (dt)/(lg-t) can be found, in which one monomer conserves its conformation. The MP2/6-311+G* calculation even predicts such a structure to be by far the global minimum structure, but this must be viewed together with the failure of this level to predict the correct Ac-Gly-OEt monomer and is therefore less likely. More realistic is the B3LYP-D3 prediction

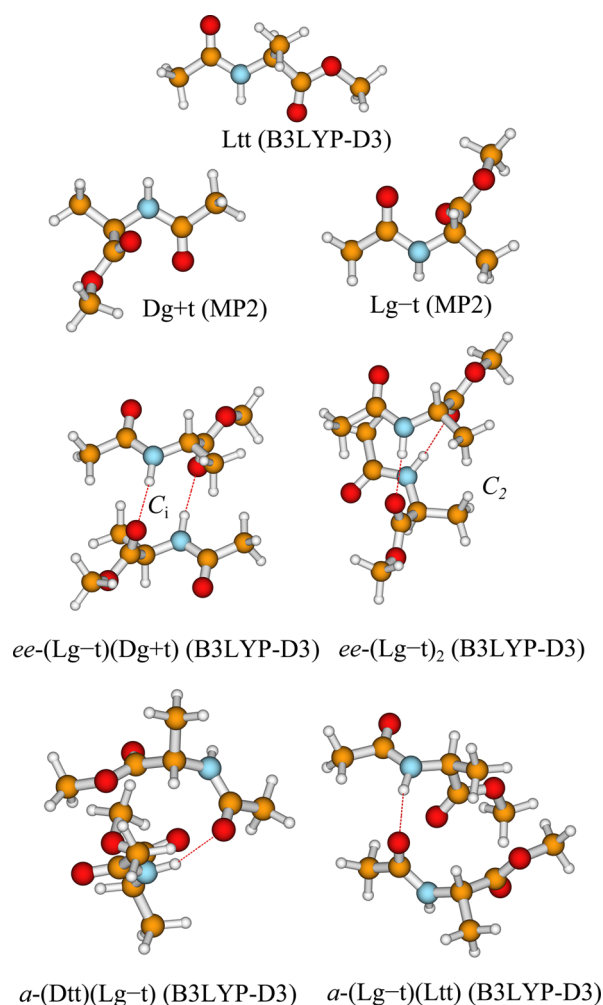


Figure 7. Ac-Ala-OMe monomer minimum structures according to B3LYP-D3 (tt) and MP2 calculations (g+t for the D-form, g-t for the L form) and the realization of the conformations in the symmetric (ee) and nonsymmetric (a) hetero- and homoconfigurational dimers.

that the unsymmetric dimer is 4 kJ mol^{-1} more stable than the C_1 symmetric one, but 2 kJ mol^{-1} less stable than the C_2 -symmetric homochiral dimer. Therefore, a switch from ee -dimers to singly amide bonded dimers is induced by a simple switch of one methyl group at the chirality center.

The observed enantiopure NH stretching spectrum (Figure 2, trace c) is indeed consistent with a dominant C_2 -symmetric structure with its strongly IR active antisymmetric NH mode and its an order of magnitude weaker and slightly more red-shifted symmetric Davydov partner. The Davydov splitting is predicted at 9 (B97D and B3LYP-D3), 7 (MP2), and 6 cm^{-1} (B3LYP), in good agreement with the experimental value of 7 cm^{-1} (Table S12 in the Supporting Information). This is also exemplified in the simulations shown in Figures 8 and 9, which assume a common dimer-to-monomer ratio of 1:5 in the NH and C=O range and single monomer (tt) and dimer ($(g-t)_2$) conformations in the enantiomerically pure case. Although the C=O shifts are in part underestimated (like for Ac-Gly-OEt), the agreement is satisfactory. Again, MP2 performs well in the NH stretching range, whereas it underestimates the ester C=O dimerization shift (Table S13 in the Supporting Information). Overall, the B3LYP-D3 spectra are most faithful to experiment, if one ignores the slight overestimate of the NH dimerization

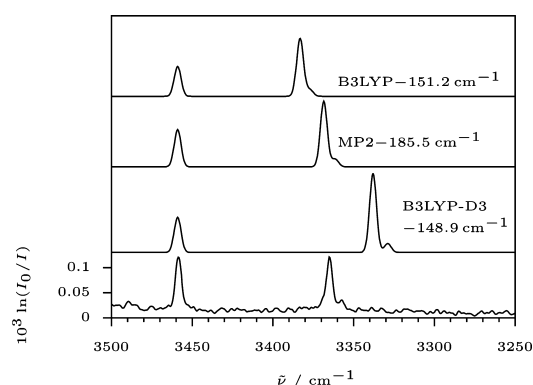


Figure 8. Simulated spectra for Ac-Ala-OMe (monomer Ltt and dimer $(lg-t)_2$ (C_2)) in the NH stretching region at the B3LYP/6-311+G*, MP2/6-311+G*, and B3LYP-D3/TZVP levels compared to the experimental spectrum (bottom trace) shown in trace c of Figure 2.

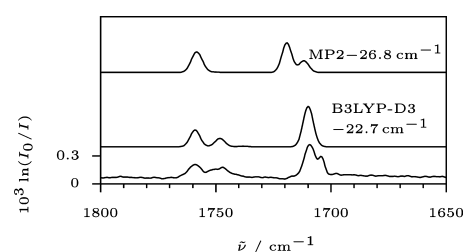


Figure 9. Simulated spectra for Ac-Ala-OMe (monomer Ltt and dimer $(lg-t)_2$ (C_2)) in the C=O stretching region at the MP2/6-311+G* and B3LYP-D3/TZVP levels compared to the experimental spectrum (bottom trace) shown in trace d of Figure 3.

shifts. This extends into the fingerprint range, where the three pronounced dimer peaks marked D in Figure 3 are well reproduced (Figure S11, Supporting Information). Turning now to the racemic spectrum (trace d in Figure 2 and trace e in Figure 3), everything points to a substantially reduced contribution of ester C=O bound dimers basically down to the 50% level expected on statistical grounds. The decrease of the Davydov shoulder at 3358 cm^{-1} could be explained by C_1 symmetry of the heterochiral dimer, but the presence of a sharp amide C=O stretching peak at 1690 cm^{-1} is more consistent with the nonsymmetric $(dtt)/(lg-t)$ or $\beta_D \epsilon_L$ dimer, which is predicted to be more stable. This is illustrated in Figure 10,

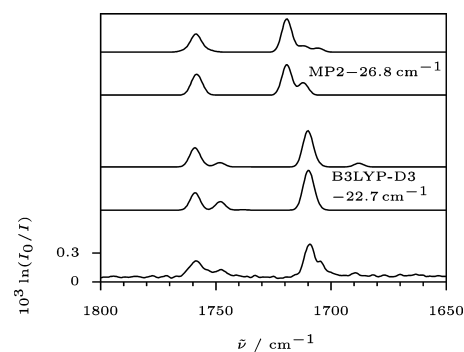


Figure 10. Simulated spectra for racemic Ac-Ala-OMe (monomer Ltt-t + and dimers $ee-(lg-t)_2$, $ee-(lg-t)/(dg+t)$ (C_1), lower trace or $a-(dtt)/(lg-t)$, upper trace) in the C=O stretching region at the MP2/6-311+G* and the B3LYP-D3/TZVP level compared to the experimental spectrum (bottom trace) shown in trace e of Figure 3.

which simulates the combined contributions of the most stable monomer and the most stable homochiral and heterochiral dimers, switching between the C_1 and the amide $C=O$ bound dimer in the latter case (Tables S15 and S16 in the Supporting Information). The preference for amide bonding also explains the decreased NH stretching intensities in the racemic expansion (Figure S10, Supporting Information).

Further evidence for the chirality-induced topology switch is provided by the simulated 1000–2000 cm^{-1} spectra (Figure S12, Supporting Information). Although the comparison of C_2 and C_1 ee -dimers reveals no significant spectral differences (Figure S12, Supporting Information), the comparison of the homochiral ee -dimer with the heterochiral a -dimer shows characteristic deviations at the positions found experimentally (Figure 3d/e). We plan to study the differences in more detail via Raman spectroscopy.

In summary, the C_2 -symmetric homoconfigurational Ac-Ala-OMe dimer is more stable than any heteroconfigurational one and the best heteroconfigurational dimer may have a different singly hydrogen-bonded topology. It has a poor spectroscopic visibility against a background of homochiral dimers but fits all quantum chemical predictions except for B97D. This remarkable switch and the subtle failure of B97D calculations to reproduce it is summarized in Figure 11. On the left side, the large gap between ee and a structures for the homochiral LL dimer is emphasized. Whereas ee structures become progressively less stable by removing (glycine) and reinserting (DL) the chirogenic methyl group, a $\beta\epsilon$ amide-bonded structure emerges for glycine and gains in relative stability for the DL alanine dimer. The qualitative deficiency of B97D seems to be a consistent stability underestimation of this $\beta\epsilon$ structure by a few kJ mol^{-1} . B3LYP-D3 may actually overestimate its stability by a small amount (see glycine), but it correctly predicts the LL \rightarrow DL switch for protected alanine.

Finally, a comparison of Ac-Ala-OMe with the well-studied phenyl-substituted Ac-Phe-OMe^{2,3} is appropriate. The monomer NH and $C=O$ fundamentals only differ by 1–4 cm^{-1} . The largest deviation (+4 cm^{-1}) is observed for the ester $C=O$ stretching mode. Monomer–dimer shifts are also within 1 cm^{-1} , except for the amide $C=O$ stretching mode, which hardly changes for Ac-Phe-OMe, whereas it red-shifts by 4 cm^{-1} for Ac-Ala-OMe. However, such small shifts are difficult to quantify for the non-size-selective FTIR technique. Therefore, the spectral evidence provides no hint for a different dimer structure in the two compounds, although the phenyl rings are likely to interact. Hence, it will be particularly rewarding to study the heterochiral dimer of Ac-Phe-OMe.

3.5. Protected Dialanine Monomer. Taking Ac-Ala-OMe as a well-characterized reference, we can move to the next-higher homologue Ac-Ala-Ala-OMe (Figure S13, Supporting Information). Its gas phase (at 413 K) and monomer-dominated jet spectra in the NH stretching range are shown in Figure 13. The gas phase (trace a) reveals a dominant absorption with a blue-shifted shoulder as well as a weaker peak at lower wavenumber. Jet cooling (trace b) resolves the main peak (M) into two features (3442 and 3436 cm^{-1}) and removes the weaker features, which are presumably due to less stable conformations. A new absorption at 3336 cm^{-1} (D) disappears in the spectrum recorded immediately after closing the valve (trace c), ruling out a monomer contribution. This points to a single dominant monomer conformation in the expansion, because Ac-Ala-Ala-OMe contains two NH stretching modes. Comparison to the six most stable monomer conformations at

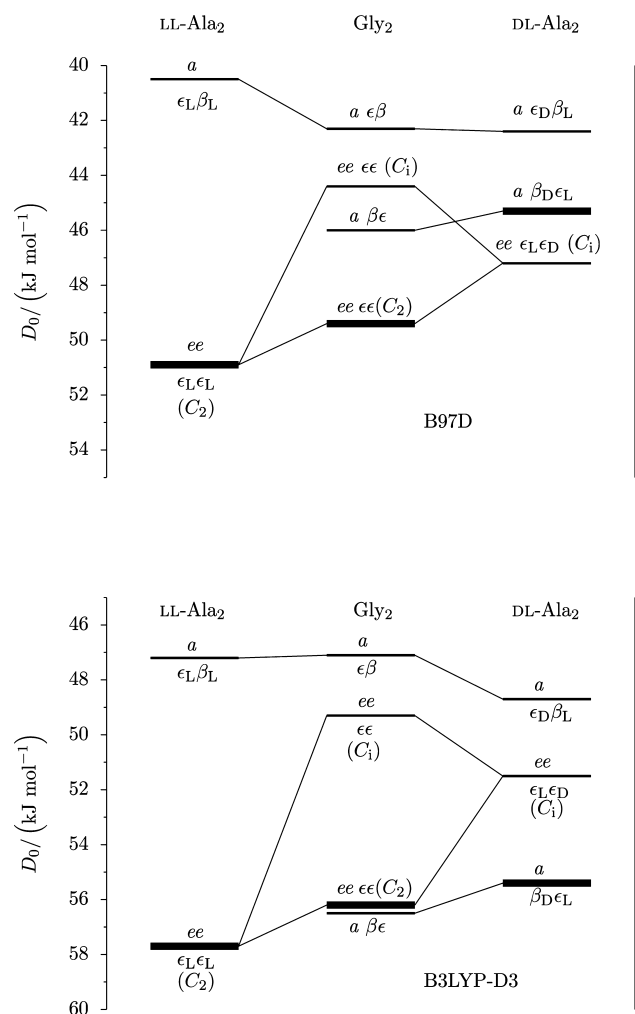


Figure 11. Switch between a symmetric ester hydrogen bonded structure for the LL alanine model dimer to the unsymmetric amide hydrogen bonded structure for the DL dimer via a balanced situation in the glycine model dimer at the B97D/TZVP (upper panel) and B3LYP-D3/TZVP (lower panel) levels. Experimentally confirmed levels are shown as bold bars.

the B3LYP-D3 level (Figure 12) shows unambiguously that this is the all-*trans* or $\beta_1\beta_L$ conformation (upper of six stick spectra in Figure 13). Note that the theoretical spectra are shifted exactly by the amount required in Ac-Ala-OMe (−148.9 cm^{-1}), avoiding introduction of any new empirical element. This adds to the confidence in the assignment. The predicted NH intensity pattern is slightly inverted with respect to experiment but well within the expected accuracy. B3LYP, B97D, and MP2 predictions are qualitatively the same and all agree in assigning the lower frequency peak to the central amide NH stretch. Depending on the level of calculation, more or less in-phase acetyl amide stretch is mixed in.

The spectral region from 1800 to 1400 cm^{-1} confirms this assignment, as shown in Figure 14. Like in the case of Ac-Ala-OMe, the central amide $C=O$ (a_m) band is substantially blue-shifted in the gas phase due to thermal weakening of the C_5 interaction in which it is involved. The intensity pattern of a strong amide $C=O$ (a_m , 1693 cm^{-1}), a weaker blue-shifted ester $C=O$ (e , 1756 cm^{-1}), and a very weak intermediate acetyl group $C=O$ (a_c , 1710 cm^{-1}) stretch is well reproduced in the theoretical all-*trans* simulation. The latter reveals that the

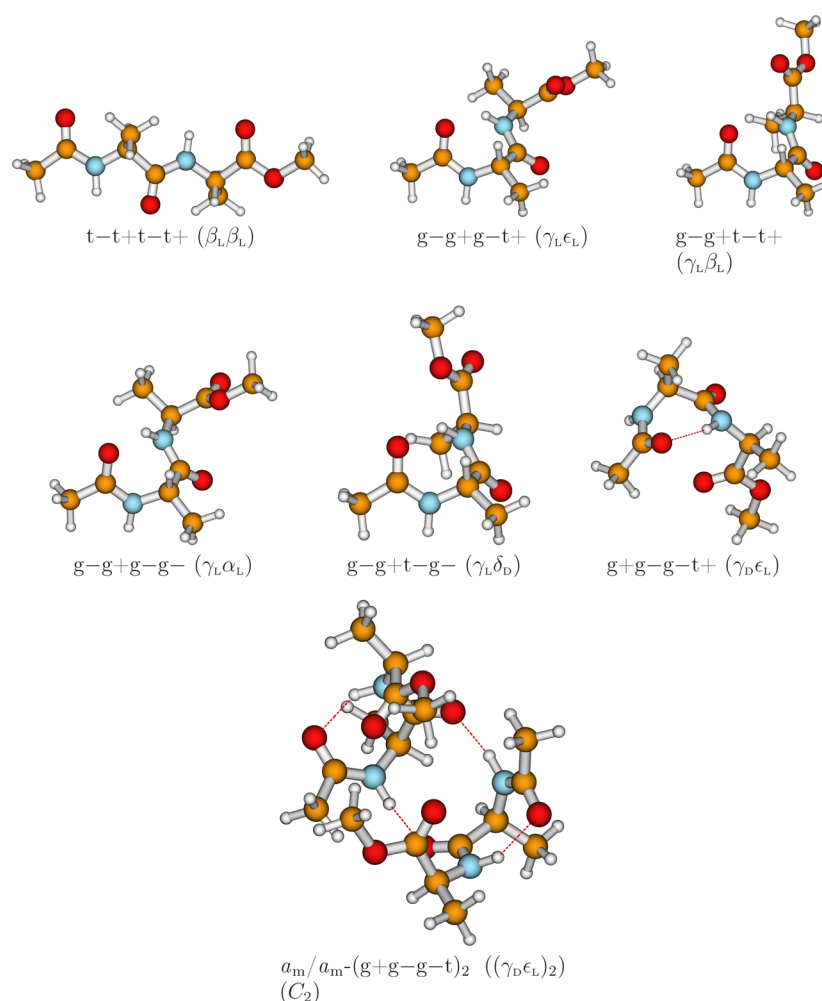


Figure 12. Ac-Ala-Ala-OMe monomer minimum structures and the most stable dimer according to B3LYP-D3 calculations.

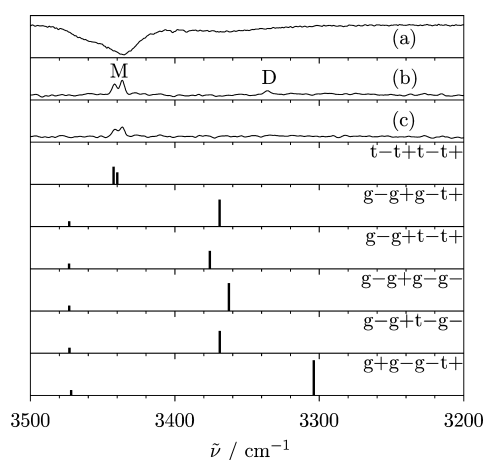


Figure 13. Experimental and calculated infrared spectra of Ac-Ala-Ala-OMe in the NH stretching region: (a) gas phase transmittance spectrum at 413 K; (b) jet spectrum, 900 jet pulses, $T_{\text{substance}} = 443$ K; (c) jet spectrum shortly after closing the magnetic valves, 900 jet pulses, $T_{\text{substance}} = 443$ K. Stick spectra of different monomers at the B3LYP-D3/TZVP level shifted by -148.9 cm^{-1} as in the Ac-Ala-OMe case.

a_m vibration gains IR intensity by mixing in some out of phase a_c motion, whereas the a_c vibration loses intensity by mixing in some in-phase a_m amplitude. This special combination is only

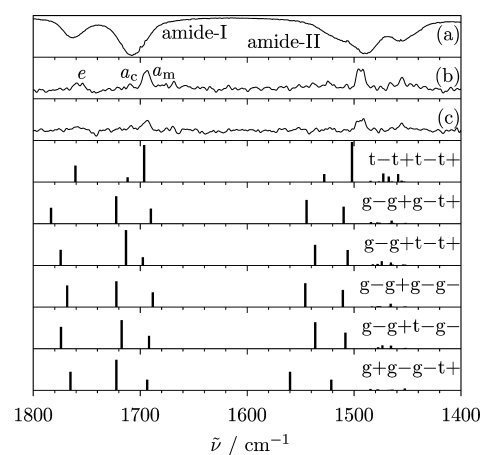


Figure 14. Experimental and calculated infrared spectra of Ac-Ala-Ala-OMe in the C=O region: (a) gas phase transmittance spectrum at 413 K; (b) jet spectrum, 1000 jet pulses, $T_{\text{substance}} = 438\text{--}443$ K; (c) jet spectrum shortly after closing the magnetic valves, 1000 jet pulses, $T_{\text{substance}} = 438\text{--}443$ K. Stick spectra of different monomers at the B3LYP-D3 level shifted by -22.7 cm^{-1} as in the Ac-Ala-OMe case. The three carbonyl groups are labeled a_c (acetyl), a_m (amide), and e (ester).

possible in the roughly planar all-*trans* conformation, further confirming our assignment. None of the C=O overtones is

predicted near the observed NH stretching bands, consistent with the observed absence of Fermi resonance interaction. Finally, the amide-II region is predicted at somewhat higher wavenumber than observed, because it involves anharmonic N–H bending motion. Again, the all-*trans* conformation is unique in reproducing the strongest intensity for the lower frequency (predominantly acetyl) NH bending mode, whereas the band near 1450 cm^{-1} has predominantly CH bending character.

The spectroscopic finding of a single dominant conformation at low temperature is in excellent agreement with earlier findings for Ac-Val-Phe-OMe¹⁶ but contrasts with most theoretical predictions. Only the B3LYP and to lesser degree the B3LYP-D3 predictions (Table S17, Supporting Information) confirm this preference. At the MP2 level, there are five folded conformations within ± 1 kJ mol^{-1} of the stretched conformation, partly as a consequence of using a small triple- ζ basis set. All these conformations include a γ turn, which switches on a C_7 hydrogen bond motif. More surprising is the qualitative failure of the B97D calculations, which predict three conformations within a 1 kJ mol^{-1} window and another two within 3 kJ mol^{-1} of the lowest structure. Even the global minimum structure is predicted to involve a γ turn. The small size of the Ala-Ala model system brings a systematic study including higher level treatments into reach. It may turn out to be a rigorous testing case between different density functionals and dispersion corrections, as the experimental $\beta_1\beta_L$ preference is unambiguous.

3.6. Protected Dialanine Dimer. In the absence of a reliable quantum chemical method to describe the monomers, firm statements about Ac-Ala-Ala-OMe dimers are difficult. Experimentally, there is a single NH stretching band at 3336 cm^{-1} (marked D in Figure 13), which can be attributed to such a dimer. It is red-shifted 29 cm^{-1} compared to the corresponding Ac-Ala-OMe dimer band. Because there are four NH stretching modes in such a dimer, it is expected to have a high symmetry and two strong intermolecular hydrogen bonds, leading to a single strongly IR active mode. We could only find one dimer structure that fulfills these constraints in a reasonable way (Table S19, Supporting Information). It consists of two g+g–g–t or $\gamma_D\epsilon_L$ monomers with an intramolecular C_7 connection between the a_c carbonyl group and the central amide NH group. This leaves the central a_m carbonyl and the acetylated amide group for strong intermolecular C_{10} hydrogen bonding in a C_2 -symmetric dimer (Figure 12). The antisymmetric acetylated amide stretch gives rise to the strongest band (predicted red-shifted 40–70 cm^{-1} relative to Ac-Ala-OMe dimer in the calculations), whereas the C_7 hydrogen bonded NH is predicted more than a factor of 2 weaker in intensity and may thus be hidden in the noise at the lower end of the spectrum. All other dimers either yield two strongly visible NH stretching bands or predict them in the wrong position. Rewardingly, the preferred structure is the lowest energy structure we could locate on the potential energy hypersurface, with a B3LYP-D3 binding energy of 85 kJ mol^{-1} after harmonic zero point energy correction (Table S18, Supporting Information). It represents another case of adaptive aggregation, with six out of eight backbone torsional angles changing from t to g. Part of the driving force for this dimer is the optimal arrangement of the two ester moieties in terms of weak C=O–methyl contacts. However, the all-*trans* dimer is energetically very close. The observed dimer concentration (at most 3% of the monomer concentration based on predicted

intensities) is too low to expect significant spectral dimer features in the carbonyl and fingerprint regions, leaving the assignment in a tentative state.

4. CONCLUSIONS

The protected amino acids Ac-Gly-OEt and Ac-Ala-OMe are confirmed to prefer stretched (tt or β) monomer conformations in the gas phase, although the dihedral angle ϕ between the amide group and the C_α ester group is rather soft and MP2 calculations with small triple- ζ basis sets predict folding around this torsional degree of freedom to be energetically feasible or even favorable. When the compounds dimerize, this folding becomes reality and the NH groups form intermolecular hydrogen bonds with the ester C=O groups. The resulting C_2 -symmetric β -sheet-like dimers are presumably global minima on the complex potential energy hypersurface although quantum chemical predictions show large variations. This homochiral pairing preference by folding appears rather different from the corresponding rigid phenylalanine behavior.^{2,3} Combination of left- and right-handed Ac-Ala-OMe appears to lead to a rearrangement of the hydrogen bond pattern, according to subtle but multiple IR spectroscopic evidence. Instead of a β -sheet-like symmetric aggregation via ester C=O hydrogen bonds, a single NH \cdots O=C hydrogen bond to amide C=O may be preferred. Final proof could come from Raman jet spectroscopy. Chirality inversion may turn out to be β -sheet breaking. However, the dimerization energy is less than in the homoconfigurational dimer case. The homochiral pairing preference of Ac-Ala-OMe is also observed in the racemic crystal, which consists of infinite chains with 2:1 alternation of L and D units.⁷³ However, the dominant hydrogen bonds in the crystal involve the amide C=O, rather than the ester C=O group.

Even the protected dipeptide Ac-Ala-Ala-OMe prefers a stretched conformation according to the experimental spectra, although calculations including dispersion interactions predict strong competition by folded conformations. Upon dimerization, this changes dramatically and a triply folded monomer structure appears to be the most stable complex. The comparison between experiment and theory reveals that B3LYP calculations show the best overall performance, if augmented by D3 dispersion corrections. B97D, apart from overestimating hydrogen bond shifts and underestimating the force constants of chemical bonds, fails in predicting some conformational details and chirality recognition effects. On the basis of this work, one can now quantify anharmonic effects for such peptide model systems.⁷⁴

It will be interesting to move to the next level of complexity, namely acetylated amides of simple nonaromatic amino acids,⁵ using the heated gas phase and supersonic jet FTIR approaches. For aromatic amino acids,² complementary Raman jet spectra may now be feasible.³⁶ One can anticipate that conformational diversity will increase, as will chirality recognition²⁸ when the C_α configuration is switched.

■ ASSOCIATED CONTENT

Supporting Information

Tables of naming conventions, relative and dissociation energies, and NH and CO stretching wavenumbers. Figures of IR spectra, simulated and experimental IR spectra, conformations, and torsion angles. This material is available free of charge via the Internet at <http://pubs.acs.org>.

AUTHOR INFORMATION

Corresponding Author

*E-mail: M.A.S., msuhm@gwdg.de; M.G., gerhards@chemie.uni-kl.de.

Present Addresses

[†]Federal Institute for Materials Research and Testing (BAM), Richard-Willstätter-Str. 11, 12489 Berlin, Germany.

[‡]Department of Chemistry, University of Basel, CH-4056 Basel, Switzerland.

Notes

The authors declare no competing financial interest.

ACKNOWLEDGMENTS

The present work was supported by the Fonds der Chemischen Industrie (Kekulé Ph.D. scholarship for J.J.L.) and by the DFG research training group 782 (www.pcgg.de).

REFERENCES

- (1) Kaminski, G. A.; Friesner, R. A.; Tirado-Rives, J.; Jorgensen, W. L. Evaluation and Reparametrization of the OPLS-AA Force Field for Proteins via Comparison with Accurate Quantum Chemical Calculations on Peptides. *J. Phys. Chem. B* **2001**, *105*, 6474–6487.
- (2) Gerhards, M.; Unterberg, C. Structures of the Protected Amino Acid Ac–Phe–OMe and Its Dimer: A β -Sheet Model System in the Gas Phase. *Phys. Chem. Chem. Phys.* **2002**, *4*, 1760–1765.
- (3) Gerhards, M.; Unterberg, C.; Gerlach, A. Structure of a β -Sheet Model System in the Gas Phase: Analysis of the C=O Stretching Vibrations. *Phys. Chem. Chem. Phys.* **2002**, *4*, 5563–5565.
- (4) Dian, B. C.; Longarte, A.; Mercier, S.; Evans, D. A.; Wales, D. J.; Zwier, T. S. The Infrared and Ultraviolet Spectra of Single Conformations of Methyl-Capped Dipeptides: N-Acetyl Tryptophan Amide and N-Acetyl Tryptophan Methyl Amide. *J. Chem. Phys.* **2002**, *117*, 10688–10702.
- (5) Gerhards, M.; Unterberg, C.; Gerlach, A.; Jansen, A. β -Sheet Model Systems in the Gas Phase: Structures and Vibrations of Ac–Phe–NHMe and Its Dimer (Ac–Phe–NHMe)₂. *Phys. Chem. Chem. Phys.* **2004**, *6*, 2682–2690.
- (6) Fricke, H.; Gerlach, A.; Gerhards, M. Structure of a β -Sheet Model System in the Gas Phase: Analysis of the Fingerprint Region Up to 10 μm . *Phys. Chem. Chem. Phys.* **2006**, *8*, 1660–1662.
- (7) De Wael, K.; Zeegers-Huyskens, T. FT-IR Study of the Proton Acceptor Ability of Ethylacetamidoacetate. Self-Association and Interaction with Proton Donors. *Spectrosc. Lett.* **1993**, *26*, 1939–1951.
- (8) Pohl, G.; Perczel, A.; Vass, E.; Magyarfalvi, G.; Tarczay, G. A Matrix Isolation Study on Ac-Gly-NHMe and Ac-L-Ala-NHMe, the Simplest Chiral and Achiral Building Blocks of Peptides and Proteins. *Phys. Chem. Chem. Phys.* **2007**, *9*, 4698–4708.
- (9) Alkorta, I.; Elguero, J. Theoretical Study of Peptide Model Dimers. Homo versus Heterochiral Complexes. *THEOCHEM* **2004**, *680*, 191–198.
- (10) Emmeluth, C.; Dyczmons, V.; Kinzel, T.; Botschwina, P.; Suhm, M. A.; Yáñez, M. Combined Jet Relaxation and Quantum Chemical Study of the Pairing Preferences of Ethanol. *Phys. Chem. Chem. Phys.* **2005**, *7*, 991–997.
- (11) Reva, I. D.; Jesus, A. J. L.; Rosado, M. T. S.; Fausto, R.; Eusébio, M. E.; Redinha, J. S. Stepwise Conformational Cooling Towards a Single Isomeric State in the Four Internal Rotors System 1,2-Butanediol. *Phys. Chem. Chem. Phys.* **2006**, *8*, 5339–5349.
- (12) Rizzo, T. R.; Park, Y. D.; Peteanu, L. A.; Levy, D. H. The Electronic Spectrum of the Amino Acid Tryptophan in the Gas Phase. *J. Chem. Phys.* **1986**, *84*, 2534–2541.
- (13) Piuze, F.; Dimicoli, I.; Mons, M.; Tardivel, B.; Zhao, Q. A Simple Laser Vaporization Source for Thermally Fragile Molecules Coupled to a Supersonic Expansion: Application to the Spectroscopy of Tryptophan. *Chem. Phys. Lett.* **2000**, *320*, 282–288.
- (14) Snoek, L. C.; Robertson, E. G.; Kroemer, R. T.; Simons, J. P. Conformational Landscapes in Amino Acids: Infrared and Ultraviolet Ion-Dip Spectroscopy of Phenylalanine in the Gas Phase. *Chem. Phys. Lett.* **2000**, *321*, 49–56.
- (15) Snoek, L. C.; Kroemer, R. T.; Simons, J. P. A Spectroscopic and Computational Exploration of Tryptophan-Water Cluster Structures in the Gas Phase. *Phys. Chem. Chem. Phys.* **2002**, *4*, 2130–2139.
- (16) Unterberg, C.; Gerlach, A.; Schrader, T.; Gerhards, M. Structure of the Protected Dipeptide Ac-Val-Phe-OMe in the Gas Phase: Towards a β -Sheet Model System. *J. Chem. Phys.* **2003**, *118*, 8296–8300.
- (17) Çarçabal, P.; Kroemer, R. T.; Snoek, L. C.; Simons, J. P.; Bakker, J. M.; Compagnon, I.; Meijer, G.; von Helden, G. Hydrated Complexes of Tryptophan: Ion Dip Infrared Spectroscopy in the ‘Molecular Fingerprint’ Region, 100–2000 cm^{-1} . *Phys. Chem. Chem. Phys.* **2004**, *6*, 4546–4552.
- (18) Chin, W.; Piuze, F.; Dognon, J.-P.; Dimicoli, I.; Tardivel, B.; Mons, M. Gas Phase Formation of a ₃₁₀-Helix in a Three-Residue Peptide Chain: Role of Side Chain-Backbone Interactions As Evidenced by IR-UV Double Resonance Experiments. *J. Am. Chem. Soc.* **2005**, *127*, 11900–11901.
- (19) Abo-Riziq, A. G.; Bushnell, J. E.; Crews, B.; Callahan, M. P.; Grace, L.; De Vries, M. S. Discrimination between Diastereoisomeric Dipeptides by IR-UV Double Resonance Spectroscopy and Ab Initio Calculations. *Int. J. Quantum Chem.* **2005**, *105*, 437–445.
- (20) Abo-Riziq, A. G.; Crews, B.; Bushnell, J. E.; Callahan, M. P.; De Vries, M. S. Conformational Analysis of cyclo(Phe-Ser) by UV-UV and IR-UV Double Resonance Spectroscopy and Ab Initio Calculations. *Mol. Phys.* **2005**, *103*, 1491–1495.
- (21) Abo-Riziq, A.; Crews, B. O.; Callahan, M. P.; Grace, L.; de Vries, M. S. Spectroscopy of Isolated Gramicidin Peptides. *Angew. Chem., Int. Ed.* **2006**, *45*, 5166–5169.
- (22) Compagnon, I.; Oomens, J.; Meijer, G.; von Helden, G. Mid-Infrared Spectroscopy of Protected Peptides in the Gas Phase: A Probe of the Backbone Conformation. *J. Am. Chem. Soc.* **2006**, *128*, 3592–3597.
- (23) Fricke, H.; Schäfer, G.; Schrader, T.; Gerhards, M. Secondary Structure Binding Motifs of the Jet Cooled Tetrapeptide Model Ac-Leu-Val-Tyr(Me)-NHMe. *Phys. Chem. Chem. Phys.* **2007**, *9*, 4592–4597.
- (24) Fricke, H.; Funk, A.; Schrader, T.; Gerhards, M. Investigation of Secondary Structure Elements by IR/UV Double Resonance Spectroscopy: Analysis of an Isolated β -Sheet Model System. *J. Am. Chem. Soc.* **2008**, *130*, 4692–4698.
- (25) Kim, H. M.; Han, K. Y.; Park, J.; Kim, S. K.; Kim, Z. H. Conformational Study of Jet-Cooled L-Phenylglycine. *J. Chem. Phys.* **2008**, *128*, 184313.
- (26) Baquero, E. E.; James, W. H.; Choi, S. H.; Gellman, S. H.; Zwier, T. S. Single-Conformation Ultraviolet and Infrared Spectroscopy of Model Synthetic Foldamers: β -Peptides Ac- β^3 -hPhe- β^3 -hAla-NHMe and Ac- β^3 -hAla- β^3 -hPhe-NHMe. *J. Am. Chem. Soc.* **2008**, *130*, 4795–4807.
- (27) Häber, T.; Seefeld, K.; Engler, G.; Grimme, S.; Kleinermanns, K. IR/UV Spectra and Quantum Chemical Calculations of Trp-Ser: Stacking Interactions between Backbone and Indole Side-Chain. *Phys. Chem. Chem. Phys.* **2008**, *10*, 2844–2851.
- (28) Zehnacker, A.; Suhm, M. A. Chirality Recognition between Neutral Molecules in the Gas Phase. *Angew. Chem., Int. Ed.* **2008**, *47*, 6970–6992.
- (29) Vaden, T. D.; Gowers, S. A. N.; Snoek, L. C. Infrared Spectroscopy of ‘Forbidden’ Peptide Sequences. *Phys. Chem. Chem. Phys.* **2009**, *11*, 5843–5850.
- (30) Vaden, T. D.; Gowers, S. A. N.; Snoek, L. C. Observation of β -Sheet Aggregation in a Gas-Phase Tau-Peptide Dimer. *J. Am. Chem. Soc.* **2009**, *131*, 2472–2474.
- (31) Gloaguen, E.; Pollet, R.; Piuze, F.; Tardivel, B.; Mons, M. Gas phase Folding of an (Ala)₄ Neutral Peptide Chain: Spectroscopic Evidence for the Formation of a β -Hairpin H-Bonding Pattern. *Phys. Chem. Chem. Phys.* **2009**, *11*, 11385–11388.

- (32) Gloaguen, E.; de Courcy, B.; Piquemal, J.-P.; Pilmé, J.; Parisel, O.; Pollet, R.; Biswal, H. S.; Piuze, F.; Tardivel, B.; Broquier, M.; et al. Gas-Phase Folding of a Two-Residue Model Peptide Chain: On the Importance of an Interplay between Experiment and Theory. *J. Am. Chem. Soc.* **2010**, *132*, 11860–11863.
- (33) Gloaguen, E.; Valdes, H.; Pagliarulo, F.; Pollet, R.; Tardivel, B.; Hobza, P.; Piuze, F.; Mons, M. Experimental and Theoretical Investigation of the Aromatic–Aromatic Interaction in Isolated Capped Dipeptides. *J. Phys. Chem. A* **2010**, *114*, 2973–2982.
- (34) Buchanan, E. G.; James, W. H.; Choi, S. H.; Guo, L.; Gellman, S. H.; Müller, C. W.; Zwier, T. S. Single-Conformation Infrared Spectra of Model Peptides in the Amide I and Amide II Regions: Experiment-Based Determination of Local Mode Frequencies and Inter-Mode Coupling. *J. Chem. Phys.* **2012**, *137*, 094301.
- (35) Albrecht, M.; Rice, C. A.; Suhm, M. A. Elementary Peptide Motifs in the Gas Phase: FTIR Aggregation Study of Formamide, Acetamide, *N*-Methylformamide, and *N*-Methylacetamide. *J. Phys. Chem. A* **2008**, *112*, 7530–7542.
- (36) Otto, K. E.; Hesse, S.; Wassermann, T. N.; Rice, C. A.; Suhm, M. A.; Stafforst, T.; Diederichsen, U. Temperature-Dependent Intensity Anomalies in Amino Acid Esters: Weak Hydrogen Bonds in Protected Glycine, Alanine and Valine. *Phys. Chem. Chem. Phys.* **2011**, *13*, 14119–14130.
- (37) Hesse, S.; Suhm, M. A. Conformation and Aggregation of Proline Esters and Their Aromatic Homologs: Pyramidal Vs. Planar RR'N-H in Hydrogen Bonds. *Z. Phys. Chem.* **2009**, *223*, 579–604.
- (38) Siodlak, D.; Janick, A. Conformational Properties of the Residues Connected by Ester and Methylated Amide Bonds: Theoretical and Solid State Conformational Studies. *J. Pept. Sci.* **2010**, *16*, 126–135.
- (39) Linder, R.; Seefeld, K.; Vavra, A.; Kleinermanns, K. Gas Phase Infrared Spectra of Nonaromatic Amino Acids. *Chem. Phys. Lett.* **2008**, *453*, 1–6.
- (40) Balabin, R. M. Experimental Thermodynamics of Free Glycine Conformations: The First Raman Experiment after Twenty Years of Calculations. *Phys. Chem. Chem. Phys.* **2012**, *14*, 99–103.
- (41) Albrecht, M.; Borba, A.; Le Barbu-Debus, K.; Dittrich, B.; Fausto, R.; Grimme, S.; Mahjoub, A.; Nedić, M.; Schmitt, U.; Schrader, L.; et al. Chirality Influence on the Aggregation of Methyl Mandelate. *New J. Chem.* **2010**, *34*, 1266–1285.
- (42) Le Barbu, K.; Brenner, V.; Millié, P.; Lahmani, F.; Zehnacker-Rentien, A. An Experimental and Theoretical Study of Jet-Cooled Complexes of Chiral Molecules: The Role of Dispersive Forces in Chiral Discrimination. *J. Phys. Chem. A* **1998**, *102*, 128–137.
- (43) Grimme, S. Semiempirical GGA-Type Density Functional Constructed with a Long-Range Dispersion Correction. *J. Comput. Chem.* **2006**, *27*, 1787–1799.
- (44) Grimme, S.; Antony, J.; Ehrlich, S.; Krieg, H. A Consistent and Accurate Ab Initio Parametrization of Density Functional Dispersion Correction (DFT-D) for the 94 Elements H–Pu. *J. Chem. Phys.* **2010**, *132*, 154104.
- (45) Cézard, C.; Rice, C. A.; Suhm, M. A. OH-Stretching Redshifts in Bulky Hydrogen Bonded Alcohols: Jet Spectroscopy and Modeling. *J. Phys. Chem. A* **2006**, *110*, 9839–9848.
- (46) Borba, A.; Albrecht, M.; Gómez-Zavaglia, A.; Lapinski, L.; Nowak, M. J.; Suhm, M. A.; Fausto, R. Dimer formation in Nicotinamide and Picolinamide in the Gas and Condensed Phases Probed by Infrared Spectroscopy. *Phys. Chem. Chem. Phys.* **2008**, *10*, 7010–7021.
- (47) Albrecht, M.; Zielke, P.; Rice, C. A.; Suhm, M. A. Variations of Bite Angle and Coupling Patterns in Double Hydrogen Bonds: The Case of Oxime Dimers. *J. Mol. Struct.* **2008**, *880*, 2–13.
- (48) Lee, J. J.; Hesse, S.; Suhm, M. A. Conformational Instability upon Dimerization: Prolinol. *J. Mol. Struct.* **2010**, *976*, 397–404.
- (49) Lee, C.; Yang, W.; Parr, R. G. Development of the Colle-Salvetti Correlation Energy Formula into a Functional of the Electron Density. *J. Chem. Phys.* **1988**, *37*, 785–789.
- (50) Becke, A. D. Density-Functional Thermochemistry. III. The Role of Exact Exchange. *J. Chem. Phys.* **1993**, *98*, 5648–5652.
- (51) Møller, C.; Plesset, M. S. Note on an Approximation Treatment for Many-Electron Systems. *Phys. Rev.* **1934**, *46*, 618–622.
- (52) Frisch, M. J.; Trucks, G. W.; Schlegel, H. B.; Scuseria, G. E.; Robb, M. A.; Cheeseman, J. R.; Montgomery, J. A., Jr.; Vreven, T.; Kudin, K. N.; Burant, J. C.; et al. *Gaussian 03*, Revision D.01; Gaussian, Inc.: Wallingford, CT, 2004.
- (53) Frisch, M. J.; Trucks, G. W.; Schlegel, H. B.; Scuseria, G. E.; Robb, M. A.; Cheeseman, J. R.; Scalmani, G.; Barone, V.; Mennucci, B.; Petersson, G. A.; et al. *Gaussian 09*, Revision A.02; Gaussian Inc.: Wallingford, CT, 2009.
- (54) Ahlrichs, R.; Bär, M.; Häser, M.; Horn, H.; Kölmel, C. Electronic Structure Calculations on Workstation Computers: The Program System Turbomole. *Chem. Phys. Lett.* **1989**, *162*, 165–169.
- (55) *Discovery Studio Client v2.5.5.9350*; Accelrys Software Inc., Copyright 2005–09.
- (56) Hoffmann-Ostenhof, O.; Cohn, W. E.; Braunstein, A. E.; Horecker, B. L.; Jakoby, W. B.; Karlson, P.; Keil, B.; Klyne, W.; Liébecq, C.; Webb, E. C. Abbreviations and Symbols for Description of Conformation of Polypeptide Chains (Rules Approved 1974). *Pure Appl. Chem.* **1974**, *40*, 291–308.
- (57) Perczel, A.; Angyán, J. G.; Kajtar, M.; Viviani, W.; Rivail, J.-L.; Marcocchia, J.-F.; Csizmadia, I. G. Peptide Models. 1. Topology of Selected Peptide Conformational Potential Energy Surfaces (Glycine and Alanine Derivatives). *J. Am. Chem. Soc.* **1991**, *113*, 6256–6265.
- (58) Ramachandran, G. N.; Sasisekharan, V.; Ramakrishnan, C. Molecular Structure of Polyglycine II. *Biochim. Biophys. Acta* **1966**, *112*, 168–170.
- (59) Klyne, W.; Prelog, V. Description of Steric Relationships Across Single Bonds. *Experientia* **1960**, *16*, 521–523.
- (60) Lavrich, R. J.; Hight Walker, A. R.; Plusquellic, D. F.; Kleiner, I.; Suenram, R. D.; Hougen, J. T.; Fraser, G. T. Conformational Analysis of the Jet-Cooled Peptide Mimetic Ethylacetamidoacetate from Torsion-Rotation Spectra. *J. Chem. Phys.* **2003**, *119*, 5497–5504.
- (61) Albrecht, M.; Will, J.; Suhm, M. A. Chirality Recognition in Menthol and Neomenthol: Preference for Homoconfigurational Aggregation. *Angew. Chem., Int. Ed.* **2010**, *49*, 6203–6206.
- (62) Wang, J.; Hochstrasser, R. M. Anharmonicity of Amide Modes. *J. Phys. Chem. B* **2006**, *110*, 3798.
- (63) Wassermann, T. N.; Rice, C. A.; Suhm, M. A.; Luckhaus, D. Hydrogen Bonding Lights up Overtone in Pyrazoles. *J. Chem. Phys.* **2007**, *127*, 234309.
- (64) Wang, J. Conformational Dependence of Anharmonic NH Stretch Vibration in Peptides. *Chem. Phys. Lett.* **2009**, *467*, 375–380.
- (65) Frey, J. A.; Leutwyler, S. An *Ab Initio* Benchmark Study of Hydrogen Bonded Formamide Dimers. *J. Phys. Chem. A* **2006**, *110*, 12512–12518.
- (66) Quack, M.; Stohner, J.; Willeke, M. High-Resolution Spectroscopic Studies and Theory of Parity Violation in Chiral Molecules. *Annu. Rev. Phys. Chem.* **2008**, *59*, 741–769.
- (67) Quack, M. In *Fundamental Symmetries and Symmetry Violations from High Resolution Spectroscopy*; Quack, M., Merkt, F., Eds.; Handbook of High-Resolution Spectroscopy; Wiley: Chichester, U.K., 2011; Vol. 1, Chapter 18, pp 659–722.
- (68) Plusquellic, D. F.; Kleiner, I.; Demaison, J.; Suenram, R. D.; Lavrich, R. J.; Lovas, F. J.; Fraser, G. T. The Microwave Spectrum of a Two-Top Peptide Mimetic: The *N*-Acetyl Alanine Methyl Ester Molecule. *J. Chem. Phys.* **2006**, *125*, 104312.
- (69) Plass, M.; Griehl, C.; Kolbe, A. Solvent Effect on the Conformational Behaviour of Amino Acid and Oligopeptide Derivatives. *J. Mol. Struct.* **2001**, *570*, 203–214.
- (70) Lee, M.-E.; Lee, S.; Joo, S.-W.; Cho, K.-H. Amide I Bands of Terminally Blocked Alanine in Solutions Investigated by Infrared Spectroscopy and Density Functional Theory Calculation: Hydrogen-Bonding Interactions and Solvent Effects. *J. Phys. Chem. B* **2009**, *113*, 6894–6897.
- (71) Rubtsov, I. V.; Wang, J.; Hochstrasser, R. M. Vibrational coupling between Amide-I and Amide-A Modes Revealed by Femtosecond Two Color Infrared Spectroscopy. *J. Phys. Chem. A* **2003**, *107*, 3384–3396.

(72) Ianoul, A.; Boyden, M. N.; Asher, S. A. Dependence of the Peptide Amide III Vibration on the Φ Dihedral Angle. *J. Am. Chem. Soc.* **2001**, *123*, 7433–7434.

(73) Müller, G.; Lutz, M. A Curious Case of Partial Spontaneous Resolution on Crystallization of a Racemate. The Crystal and Molecular Structures of *N*-Acetyl-DL-Alanine Methyl ester and *N*-Acetyl-L-Alanine Methyl ester. *Z. Naturforsch.* **2001**, *56 b*, 871.

(74) Kaledin, A. L.; Bowman, J. M. Full Dimensional Quantum Calculations of Vibrational Energies of *N*-Methyl Acetamide. *J. Phys. Chem. A* **2007**, *111*, 5593–5598.